Available online at www.sciencedirect.com
ScienceDirect
Journal of Nuclear Materials 363–365 (2007) 806–810
journal of nuclear materials
www.elsevier.com/locate/jnucmat

Effect of magnetic configuration on the neutral particle transport in compact helical system edge region

H. Matsuura [a,*], C. Suzuki [b], S. Okamura [b]

[a] Osaka Prefecture University, Gakuen-cho 1-1, Sakai Naka-ku, Osaka 599-8531, Japan
[b] National Institute for Fusion Science, Toki, Gifu 509-5292, Japan

Abstract

Neutral particle behavior in compact helical system (CHS) was studied with the Monte Carlo simulation code DEGAS. By shifting the magnetic axis position, magnetic configuration of CHS device changes from the material limiter to the magnetic divertor. We estimated Hα emission from excited hydrogen atoms and dissociated molecules with a collisional radiation model, and compared experimental observations to study the change of recycling condition. With the comparison of simulation result with Hα detector signal, the change of recycling source by the magnetic axis shift was qualitatively confirmed.

PACS: 52.55.Hc; 52.65.Pp

Keywords: DEGAS; Neutrals; Recycling; Edge modeling; Magnetic topology

1. Introduction

Neutral particle transport is an important issue not only to study plasma particle/energy balance but also to improve core plasma confinement. Dominant neutral particle source is due to the recycling at the first wall, limiter, and divertor plates. In devices such as Stellarator/Heliotron, the distribution of this source is localized in poloidal and/or toroidal direction, so neutral transport must be analysed three dimensionally. The DEGAS neutral transport simulation code (ver. 63) [1] has been applied to evaluate neutral density profile in large helical device (LHD) [2] and Heliotron-J [3] successfully.

In this study, we expand our simulation work on compact helical system (CHS) in National Institute for Fusion Science (NIFS) to full three-dimensional models. CHS is a low aspect ratio device and has an unique property concerning neutral recycling. By shifting the magnetic axis position along torus outward direction, magnetic configuration for the plasma confinement changes from the material limiter type to the magnetic divertor type. The latter is the same configuration such as LHD. The distribution of neutral recycling on the vacuum vessel is also expected to change with the magnetic axis shift. So we must check our simulation results with

* Corresponding author.
E-mail address: matsu@me.osakafu-u.ac.jp (H. Matsuura).

0022-3115/$ - see front matter
doi:10.1016/j.jnucmat.2007.01.222

experimental observations such as Hα detector data and improve the model with which we include the wall recycling condition.

In Section 2, we explain CHS device and our calculation geometry. In Section 3, we present some simulation results for two magnetic axis shift condition. Section 4 is the summary.

2. CHS device and model geometry

CHS is a heliotron/torsatron device with major radius of 1 m and minor radius of 0.2 m. The pole number of the helical field coil is $\ell = 2$ and toroidal periodic number is $m = 8$. Profiles of plasma density and temperature are measured with YAG Thomson scattering. The Li-beam probe is also used to edge plasma measurement [4].

On the contrary to other helical devices such as LHD, the CHS plasma in the standard magnetic configuration has contact with the inner wall like as the material limiter and the neutral recycling become dominant there. Moreover, the gap between the vacuum wall and main plasma varies along toroidal direction. For example, at the toroidal cross section with toroidal angle $\phi = 0°$, where magnetic surfaces are elongated vertically, core plasma has contact with the chamber wall inside of the torus major radius direction and the neutral recycling will occur there. But, at the other toroidal cross section with $\phi = 22.5°$, where magnetic surfaces are elongated horizontally, partial magnetic limiter configuration is established and there exists no direct contact between main plasma and the wall material.

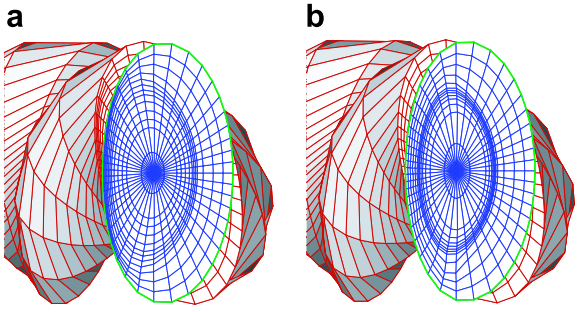

Fig. 1. Calculation geometry for the DEGAS simulation. Core plasma and vacuum region is divided into $45 \times 13 \times 48$ zones. Left figure is the standard configuration and right one is outward-shifted configuration. (a) Standard configuration model, (b) outward shifted configuration model.

Fig. 1 shows our calculation geometry for the DEGAS simulation. Core plasma and 'vacuum' region is divided into 45 zones poloidally and into 13 zones radially. Nine radial zones are determined by using KMAGN code [5]. Other four zones are interpolated between the chamber wall and the last closed flux surface (LCFS). Toroidally 48 cross sections are selected to construct the three-dimensional mesh. Fig. 1a shows our mesh model for the standard magnetic configuration, where magnetic axis position along the major radius direction is $R_{ax} = 92.1$ cm. Fig. 1b is the model for $R_{ax} = 96.2$ cm. As there is no direct contact between the wall and core plasma in the latter figure, the built-in helical divertor will work like in LHD.

Plasma parameters are assumed to be homogeneous along the poloidal/toroidal direction and assigned to each zones. This assumption must be checked carefully especially in the 'vacuum' region, since there exists cold thin SOL plasma and it may be affected by inhomogeneous magnetic field structure. Since no YAG Thomson data is available around or outside of LCFS, we set the density of 'vacuum' zones with lithium(Li)-beam probe measurement [4]. We used plasma parameters obtained from NBI heated plasma. (Heating power is about 1.5 MW and line average density of plasma center is about 2×10^{13} cm^{-3}.)

Experimental informations on neutral particles are obtained through Balmer line emission (mainly Hα). Until now, we have no Hα detectors at $\phi = 0°$ cross section, where neutral recycling with vessel wall (limiter) is expected to occur in the standard magnetic configuration. As neutral particles entering into core plasma are soon ionized and can not move long distance, their toroidal transport through the gap between chamber wall and core plasma determines the neutral density profile. If our Hα detectors sight lines oriented to neutral density peak, we obtain large signal. But if the toroidal transport changes, we may lost Hα signal. We must consider both neutral transport and detector orientation.

Up to now, we assigned only wall recycling as the neutral source. The choice of its strength and profile is very important to explain the experimental observation. Total number of test particle is several ten thousands in this work, and launched as hydrogen molecules with room temperature energy. Hydrogen atoms are produced in the interactions with core plasma. We compare the results of the simulation with different recycling condition and try to deduce which recycling model is most realistic.

3. Calculation results

3.1. Standard configuration case

In the so-called standard configuration (the material limiter), we set eight neutral particle sources at inner wall of vertically elongated toroidal cross sections ($\phi = 0°, 45°, \ldots, 315°$), since CHS helical coils have toroidal periodicity of $m = 8$. This source model is schematically shown in Fig. 2a. There is not any sink of neutral particles in this model, so we chase neutral particle flights until they are ionized in core plasma. The total intensity of sources is estimated from particle confinement time (τ_p) data. Unfortunately, experimental τ_p data is very limited. In this paper, we neglect variation of τ_p with experimental condition and used typical value of 10^{21} s^{-1} as the source intensity.

Fig. 3 shows hydrogen atomic density (n_0) profile in a half toroidal period. The poloidal cross section in Fig. 3a has recycling source on the left-hand side (inner wall) and, therefore, shows highest density among these figures. Since the absolute value of recycling neutral flux cannot be assigned exactly, calculated n_0 is relative value. Since n_0 in outer region in Fig. 3a is smaller than 10^{10} cm^{-3} and kept lower than the peak value in Fig. 3b or c (about 10^{11} cm^{-3}), neutral transport along the toroidal direction is more dominant than the poloidal direction in this configuration. Similar results is obtained also from molecular hydrogen profile.

In Fig. 4, we calculate the Hα emission profile from the atomic hydrogens profile with collisional radiation (CR) model [6]. Fig. 4a correspond to cross section ($\phi = 30.4°$) where Hα detector located at poloidal cross section named as 2O. (Here after we write as Hα detector 2O for simplicity.) Fig. 4b is for detector 8P ($\phi = 36.3°$). The sight line of each detector is plotted with solid lines. Although

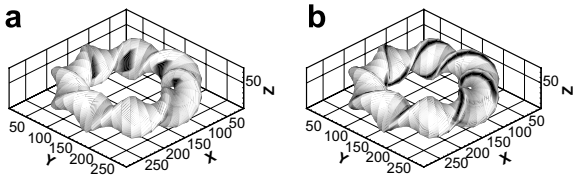

Fig. 2. Assumed hydrogen recycling distribution. In limiter source, we set eight neutral particle sources at inner wall of vertically elongated toroidal cross sections ($\phi = 0°, 45°, \ldots, 315°$). In divertor source, we assumed that recycling occurs mainly on the wall segment on which so-called divertor legs are expected to strike. (a) Limited source, (b) divertor source.

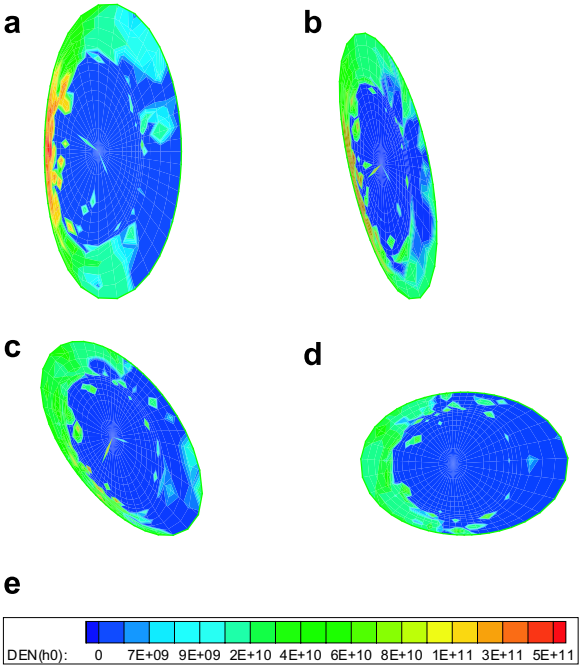

Fig. 3. Atomic hydrogen density profile for standard configuration mesh model. Four figures show neutral profile variation in a half pitch of toroidal direction. The color ruler of (e) is common for all other figures. (a) $n_H(\phi = 0.0°)$; (b) $n_H(\phi = 7.5°)$; (c) $n_H(\phi = 15.0°)$; (d) $n_H(\phi = 22.5°)$. (e) Ruler of contour (in cm^3 unit). (For interpretation of the references to colour in this figure legend, the reader is referred to the web version of this article.)

poloidal cross section of detector 8P is toroidally neighboring to particle recycling sources and has higher peak neutral density, the detector sight does not direct to this peak. On the contrary, detector 2O is looking at inner wall, where high density neutral transported from the recycling source exists, and Hα signal is expected to be large.

Though Hα emission is mainly from atomic hydrogen deeply penetrated into core plasma, contribution from molecular hydrogen is very localized around LCFS and can not neglected there. We sum up both contributions and compare for different detectors in Table 1. From the DEGAS simulation, the signal of detector 2O is expected to be larger than detector 8P by a factor of 10. Experimental data of 2O signal of Shot No. 120445 is also larger than 8P, although the signal ratio is still different between experiment and simulation.

3.2. Outward shifted configuration case

When the magnetic axis of CHS plasma shifts outward, the magnetic configuration approaches

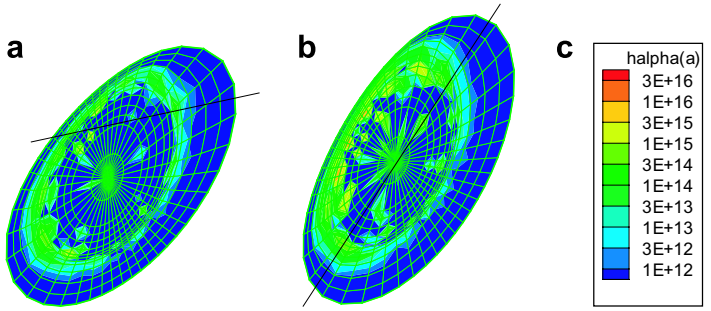

Fig. 4. Hα emission profiles for standard configuration model, calculated from DEGAS simulation results with CR model. Left figure is the cross section where 2O detector locates and right figure is for 8P. Straight lines in the figure is the sight line of each detectors. The color ruler of (c) is common for all other figures. (a) Hα(2O section); (b) Hα(8P section); (c) ruler of contour. (For interpretation of the references to colour in this figure legend, the reader is referred to the web version of this article.)

Table 1
Experiment and calculation results for Hα detectors

Ch.(tor.ang.ϕ)	2O(30.4)	2M(22.5)	8P(36.3)
EXP.(120445)	0.32	0.36	0.23
DEGAS(STD)	3.5E+15	4.1E+13	2.1E+14
EXP.(118873)	0.22	0.32	0.45
DEGAS(OUT)Lim.	1.2E+14	2.3E+13	2.9E+13
DEGAS(OUT)Div.	2.5E+14	3.2E+13	1.2E+15

Both value are written in arbitrary unit, so direct comparison between experimental value and calculation is meaningless. Shot No. 120455 was done with $R_{ax} = 92.1$ cm and Shot No. 118873 was $R_{ax} = 96.2$ cm.

to magnetic limiter (the divertor) geometry and Hα emission signals are also changed. In standard configuration (Fig. 1a), NBI heated plasma shows clear drop of Hα emission signal (for example from 2O detector) and increase of line-average density and stored energy. In $R_{ax} = 96.2$ cm case (Fig. 1b), however, we have not observed clear Hα signal drop due to edge transport barrier (ETB) formation [7]. As shown in shot No. 118873 data of Table 1, Hα emission signal ratio such as 8P signal/2O signal also changes with the magnetic axis shift.

When DEGAS simulation is done with the outward shift mesh model (Fig. 1b) and the same source model (Fig. 2a), the results, which were indicated as 'Lim.' in Table 1, are similar with the standard configuration and cannot explain experimental results. 2O signal is still larger than 8P. So we apply other neutral source model as shown in Fig. 2b. In this model, we assumed that recycling occurs mainly on the wall segment on which so-called divertor legs are expected to strike. Our knowledge on the exact distribution of CHS field line foot points, especially in toroidal direction, is very poor. So the future work combining with KMAGN code results may be necessary.

One example of simulation results with different source model is shown in Fig. 5. This is the Hα emission profile from the atomic hydrogens on cross section 8P. ($\phi = 30.4°$, same as Fig. 4b.) If the neutral recycling is divertor-like, neutral distribution is drastically changed. In this cross section, neutral density has the peak around the major axis of elliptic cross section on the chamber wall. So the signal of 8P Hα detector, whose sight is nearly parallel to major axis, becomes large in Fig. 5b, although this detector does not see the maximum Hα emission region in Fig. 5a.

Total Hα detector signal including both atomic and molecular hydrogen is shown again in Table 1. Only with divertor source model, DEGAS simulation can explain the signal intensity reversal between 2O detector and 8P detector. This qualitatively indicates that the large change of recycling source occurs by the magnetic axis shift. Since we observe establishment of ETB in the standard

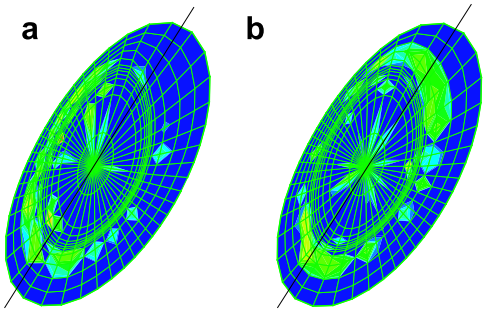

Fig. 5. Hα emission profile for outward shifted configuration model. Both figures are for 8P detector. Left figure was obtained with Fig. 2a source and right figure was with Fig. 2b. The color ruler is the same as Fig. 4. (a) Limiter source; (b) Divertor source. (For interpretation of the references to colour in this figure legend, the reader is referred to the web version of this article.)

configuration case and no ETB in this outward shifted configuration case, it is possible that the change of recycling source and neutral distribution has a relation with ETB. This means that our simulation can reproduce qualitative behavior of neutrals in CHS but must be improved to obtain quantitative results. More simulation study for other magnetic axis position will be necessary.

4. Summary

Obtained results in this paper are summarized like the following:

- 3D mesh generator was developed and DEGAS simulations on CHS was extended to include toroidal transport.
- In standard configuration (limiter), neutral particles moves long distance mainly along toroidal direction. This is due to the existence of the gap between chamber wall and core plasma.
- Hα emission profile from hydrogen molecules is very localized around LCFS compared with that from atoms.
- Even if Hα emission profile has a large peak, the direction of detector sight may miss this peak and Hα signal may be small. So, in order to examine Hα, both neutral atomic/molecular transport and detector setting must be taken into account.
- With the comparison of simulation result with Hα detector signal, the change of recycling source by the magnetic axis shift was qualitatively confirmed.

In order to compare simulation results and experimental observation quantitatively, more detail modeling of neutral source and study on other configuration will be needed. These are left for the future work.

Acknowledgements

Authors would like to thank Dr M. Shoji (NIFS) and Mr S. Iguchi (Denso Ltd.) for advices on 3D-DEGAS simulation. This work is performed with the support and under the auspices of the NIFS Collaborative Research Program.

References

[1] D. Heifetz et al., J. Comp. Phys. 46 (1982) 309.
[2] M. Shoji et al., J. Nucl. Mater. 313–316 (2003) 614.
[3] S. Kobayashi et al., 31st EPS Conf. Plasma Phys., London, (2004) ECA Vol. 28G, P-5.097.
[4] K. Nakamura et al., J. Nucl. Mater. 313-316 (2003) 725.
[5] Y. Nakamura et al., J. Plasma Fusion Res. 69 (1993) 41.
[6] T. Fujimoto et al., Nucl. Fusion 28 (1988) 1255.
[7] T. Akiyama et al., 32nd EPS Conf. Plasma Phys., Tarragona (2005) ECA Vol. 29C, P-2.070.